THE JOURNAL OF BIOLOGICAL CHEMISTRY
Vol. 279, No. 26, Issue of June 25, pp. 26868–26875, 2004

*Printed in U.S.A.*

# The Formation of Straight and Twisted Filaments from Short Tau Peptides*

Received for publication, March 2, 2004, and in revised form, April 19, 2004
Published, JBC Papers in Press, April 20, 2004, DOI 10.1074/jbc.M402379200

**Warren J. Goux‡§, Lauren Kopplin‡, Anh D. Nguyen‡, Kathryn Leak‡, Marni Rutkofsky‡, Vasanthi D. Shanmuganandam‡, Deepak Sharma¶, Hideyo Inouye¶, and Daniel A. Kirschner¶‖**

*From the ‡Department of Chemistry, the University of Texas at Dallas, Richardson, Texas 75083-0688 and the ¶Biology Department, Boston College, Chestnut Hill, Massachusetts 02467-3811*

**We studied fibril formation in a family of peptides based on PHF6 (VQIVYK), a short peptide segment found in the microtubule binding region of tau protein. *N*-Acetylated peptides AcVYK-amide (AcVYK), AcIVYK-amide (AcPHF4), AcQIVYK-amide (AcPHF5), and AcVQIVYK-amide (AcPHF6) rapidly formed straight filaments in the presence of 0.15 M NaCl, each composed of two laterally aligned protofilaments ~5 nm in width. X-ray fiber diffraction showed the omnipresent sharp 4.7-Å reflection indicating that the scattering objects are likely elongated along the hydrogen-bonding direction in a cross-$\beta$ conformation, and Fourier transform IR suggested the peptide chains were in a parallel (AcVYK, AcPHF6) or antiparallel (AcPHF4, AcPHF5) $\beta$-sheet configuration. The dipeptide *N*-acetyl-YK-amide (AcYK) formed globular structures ~200 nm to 1 $\mu$m in diameter. The polymerization rate, as measured by thioflavin S binding, increased with the length of the peptide going from AcYK → AcPHF6, and peptides that aggregated most rapidly displayed CD spectra consistent with $\beta$-sheet structure. There was a 3-fold decrease in rate when Val was substituted for Ile or Gln, nearly a 10-fold decrease when Ala was substituted for Tyr, and an increase in polymerization rate when Glu was substituted for Lys. Twisted filaments, composed of four laterally aligned protofilaments (9–19 nm width, ~90 nm half-periodicity), were formed by mixing AcPHF6 with AcVYK. Taken together these results suggest that the core of PHF6 is localized at VYK, and the interaction between small amphiphilic segments of tau may initiate nucleation and lead to filaments displaying paired helical filament morphology.**

Neurofibrillary tangles accumulate in the neurons and glia in brains of patients with several neurodegenerative diseases, including Alzheimer's disease (AD),[1] Down's syndrome, progressive supranuclear palsy, corticobasal degeneration, Pick's disease, and a number of familial frontotemporal dementias with Parkinsonism linked to chromosome 17. The frequency of their occurrence in neuronal tissue has been correlated to the progression of the disease (1–5). The neurofibrillary tangles are composed of straight filaments and paired helical filaments (PHFs), and the morphology of the PHFs is characteristic of the disease pathology. For example in AD, the PHFs appear either as twisted ribbons or pairs of protofilaments wound around one another in a left-handed helical sense with a width alternating between 10 and 20 nm and a half-periodicity of 80 nm, whereas in Pick's disease, the PHFs are slightly wider and have a half-periodicity near 200 nm (4, 6–8). However, immunological and biochemical evidence suggests that in all of the above neurodegenerative diseases the PHFs are composed of the microtubule-associated protein tau (1–4, 9, 10).

The primary structure of tau consists of an acidic N terminus containing up to two 29-amino acid inserts, a proline-rich region midway through the sequence, and a basic microtubule binding region (MTBR) containing either three or four tandem 31 (or 32)-amino acid pseudo-repeats (3R or 4R tau) near the C terminus (10–12). In AD, tau is overexpressed and contains three to four times the number of moles of phosphate as that found in normal adult tau (13–16), although the mechanistic role of phosphorylation in tau aggregation into PHFs remains unclear (17, 18).

X-ray and electron diffraction data of PHFs isolated from AD and Down's syndrome patients and of synthetic PHFs prepared from tau constructs suggest that a significant portion of the protein exists in a cross-$\beta$ conformation (19–22). Biochemical evidence suggests that three of the four pseudo-repeats making up the MTBR form the core of the PHF structure, and polymerization studies with recombinant tau show that constructs lacking these regions fail to polymerize into PHFs (23–29). It has been shown recently that that a key role in tau polymerization is the formation of $\beta$-sheet structure arising from short hexapeptide motifs in the second and third repeat of tau, $^{275}$VQIINK$^{280}$ (PHF6* in R2) and $^{306}$VQIVYK$^{311}$ (PHF6 in R3) (19, 30–32), and it has been speculated that the interaction between these two regions gives rise to the unique PHF morphology (19, 30). Although other interactions between residues distant from one another in the protein sequence have been proposed to either regulate the kinetics of tau polymerization or filament morphology (18, 26, 33–34), we chose to study the amyloid forming properties of a family of short peptides built on the PHF6 sequence. We had the following goals: 1) identify residues within the PHF6 sequence that were essential for tau

* This work was supported by an Alzheimer's Association/T. L. L. Temple Discovery award (to D. A. K.), by institutional support from Boston College, and by Grant 1R03AG16042-01 from the National Institute on Aging (to W. J. G.). The costs of publication of this article were defrayed in part by the payment of page charges. This article must therefore be hereby marked "*advertisement*" in accordance with 18 U.S.C. Section 1734 solely to indicate this fact.

§ To whom correspondence should be addressed: The University of Texas at Dallas, P. O. Box 830688, Richardson, TX 75083-0688. Tel.: 972-883-2660; Fax: 972-883-2925; E-mail: wgoux@utdallas.edu.

‖ Recipient of a Fulbright Senior Research Scholar Award from the Binational United States-Italian Fulbright Scholar Program.

[1] The abbreviations used are: AD, Alzheimer's disease; PHFs, paired helical filaments; MTBR, microtubule binding region of tau protein; R2, R3, or R4, the second, third or fourth repeat motif of the tau microtubule binding region; 3R, 4R, tau protein or peptides containing three or four repeat regions; HFIP, hexafluoroisopropanol; MOPS, 3-(*N*-morpholino)propanesulfonic acid; ThS, thioflavin S; Ac, acetyl group; TEM, transmission electron microscopy; FTIR, Fourier transform IR.

polymerization; 2) determine whether sequences in other regions of the protein might also act as nuclei for PHF formation; and 3) test if interactions between short tau peptides could lead to PHF formation.

While undertaking this work we discovered that amyloid filaments could be prepared from *N*-acetyl-Val-Tyr-Lys-amide (AcVYK) tripeptide and that spherical and globular structures, similar to prefilament structures observed in other amyloid-forming proteins (33, 35–41), could be prepared from the dipeptide *N*-acetyl Tyr-Lys-amide (AcYK). To our knowledge these are the smallest peptides to date from which amyloid or preamyloid structures have been prepared. We also found that PHF-like filaments could be prepared from a mixture of *N*-acetyl-PHF6-amide (AcPHF6) and AcVYK. These findings suggest that the core structure of PHF6 is localized at VYK, and the interaction between very small amphiphilic segments of tau may initiate nucleation and lead to filaments displaying PHF morphology.

## EXPERIMENTAL PROCEDURES

*Peptides*—PHF6 (VQIVYK), AcPHF5 (Ac-QIVYK-amide), AcPHF4 (Ac-IVYK-amide), and AcVYK (Ac-VYK-amide) were purchased from the Core Lab Facility, Department of Physiology, Tufts University (Boston). AcPHF6 (Ac-VQIVYK-amide) was purchased from Macromolecular Resources (Ft. Collins, CO). Peptides AcPHF6IV (Ac-VQVVYK-amide), AcPHF6YA (Ac-VQIVAK-amide), AcPHF6QV (Ac-VVIVYK-amide), AcPHF6KE (Ac-VQIVYE-amide), and AcYK (Ac-YK-amide) were synthesized by using Fmoc (*N*-(9-fluorenyl)methoxycarbonyl)-protected amino acids and standard solid-phase synthetic methodologies (42). Acetylation of the N terminus was accomplished by using acetic anhydride and pyridine. Peptides were dissolved in 1:1 formic acid (99%), hexafluoroisopropanol (HFIP), filtered through a 0.4-$\mu$m filter and purified with reverse-phase high pressure liquid chromatography using a gradient of 0% acetonitrile to 75% acetonitrile over 30 min. Both the water and the acetonitrile contained 0.1% trifluoroacetic acid. The purified peptides were lyophilized, and their identity was confirmed by using matrix-assisted laser desorption/ionization mass spectroscopy. Observed and calculated molecular weights are summarized in Table I.

*Transmission Electron Microscopy (TEM)*—All peptides were dissolved in either 5 or 20 mM MOPS buffer, pH 7.2. Except for AcYK, the final concentration of the peptide monomer was between 0.1 and 1 mg/ml. The AcYK sample was prepared by dissolving 4.4 mg of the peptide in 1 ml of 5 mM MOPS containing 0.15 M NaCl. Mixtures of AcVYK and AcPHF6 peptides were prepared by mixing equal volumes of freshly prepared 5 mM MOPS-buffered solutions of AcPHF6 (0.5 mg/ml) and AcVYK (0.65 mg/ml). Unless otherwise stated, samples were aged at least 2 days at room temperature (~21 °C) prior to TEM.

Samples for TEM were prepared by floating a Formvar carbon-coated copper grid on a 10-$\mu$l drop of the sample for 10 min. The sample was then negatively stained for 2 min with 1% uranyl acetate, rinsed one time with deionized water, and wicked dry. A JEOL 1200 EX scope interfaced to a digital camera was used to visualize samples.

*Far-UV CD*—Lyophilized peptides were dissolved in 5 mM MOPS to a final concentration of 0.5–1 mg/ml. Concentrations determined by weight, assuming the trifluoroacetic acid salt of the purified peptide, agreed within 5% of concentrations determined using the reported molar extinction coefficients for tyrosine ($\epsilon_{276}$ of 1390 $M^{-1}$ $cm^{-1}$ (43)) or for the peptide bond ($\epsilon_{192}$ of 7110 $M^{-1}$ $cm^{-1}$ (44)).

CD spectra were acquired on an AVIV model 202 spectropolarimeter using a cylindrical quartz cell with a 0.2-mm path length. Temperature was controlled at 20 °C by using an electrothermal cell holder. Spectra were scanned between 250 and 180 nm with a spectral resolution of 1 nm and an averaging time of 2 s per data point. The spectra reported represent an average of four acquisitions and have been smoothed using boxcar averaging (5-data point average).

*FTIR Measurements*—Lyophilized samples, except for AcPHF6KE, were dissolved in deuterium oxide ($D_2O$) to a concentration of ~10 mg/ml and allowed to stand at room temperature for 2–14 days prior to spectral acquisition. This aging period allowed for deuterium exchange of the amide backbone hydrogens and formation of filaments. Spectra were obtained by placing 25 $\mu$l of sample between two $CaF_2$ plates separated by a 20-$\mu$m Teflon spacer. IR spectra of AcPHF6KE, a peptide insoluble in $D_2O$, were obtained by dissolving the peptide in HFIP and allowing the solution to dry onto the $CaF_2$ plates. All FTIR spectra were acquired on a Nicolet Avatar 360 FTIR at 2 $cm^{-1}$ resolution by averaging 128 transients and subtracting a background spectrum of $D_2O$. Spectra were fit by Gaussian functions using nonlinear deconvolution software (Peakfit®, Systat, Richmond, CA).

*Kinetics*—Polymerization of tau peptides in solutions containing 20 mM MOPS, pH 7.2, and 0.15 M NaCl was measured by following the increase in fluorescence of thioflavin S (ThS) upon its binding to aggregated peptide species (45–47). Polymerization was initiated by the addition of 1–5 $\mu$l of 1 M NaCl to a solution containing 2.2 $\mu$M peptide and 10 $\mu$M ThS. Fluorescence was followed at 480 nm with excitation at 440 nm using 5 nm excitation and emission slit widths. All measurements were carried out at 21 °C with an LS50B spectrofluorimeter (PerkinElmer Life Sciences) using a 75-$\mu$l quartz cell. Data points were collected at 1-s intervals over the course of the experiment (1200–7000 s). Apparent first-order rate constants were estimated by fitting the base-line corrected data to a single exponential, consistent with a seeded nucleation-elongation mechanism (45–48). A two-parameter fit was carried out by using Equation 1,

$$\frac{I_t - I_0}{I_f - I_0} = (1 - e^{-k_1 t}) \qquad \text{(Eq. 1)}$$

where $I_t$ and $I_f$ are the fluorescence intensities at time $t$ and at equilibrium; $k_1$ is the apparent first-order rate constant. $I_f$ and $k_1$ were treated as adjustable parameters and fit to the first 2000 data points.

*X-ray Diffraction*—The sample peptides were analyzed under different conditions: lyophilized, vapor-hydrated, and solubilized then dried. For the first condition, the lyophilized peptide was gently packed into a thin-walled siliconized glass capillary (0.7 mm diameter; Charles A. Supper Co., South Natick, MA) to form a disk. The vapor-hydrated sample was prepared by equilibrating lyophilized peptide against water vapor in a sealed capillary tube. For preparing solubilized/dried peptide assemblies, lyophilized peptide was dissolved at ~5–10 mg/ml in water, loaded into capillary tubes, and then allowed gradually to dry at ambient temperature and humidity while in a 2-Tesla permanent magnet (Charles A. Supper Co.), which can promote fibril alignment by diamagnetic anisotropy of peptide bonds and aromatic groups (49, 50). After the peptide solution dried to a small, uniform disk, the capillary tube was removed from the magnetic field and transferred to the sample holder for x-ray diffraction.

The x-ray diffraction patterns were obtained by using nickel-filtered, double-mirror focused $CuK_\alpha$ radiation from an Elliott GX20 rotating anode x-ray generator (GEC Avionics, Hertfordshire, UK) with a 200-$\mu$m focal spot, operated at 35 kV and 35 mA. A helium tunnel was placed in the x-ray path to reduce air scatter. Patterns were recorded on DEF films (Eastman Kodak). The known Bragg spacing of calcite (3.035 Å) was used to calibrate the specimen-to-film distance (87.4 mm). The Bragg spacings of reflections were measured directly from the film or from densitometer tracings of the x-ray films.

## RESULTS

*Tau-related Peptides Used in This Study*—The peptides studied were analogs of PHF6 (VQIVYK), a peptide homologous to a segment within the third MTBR of tau (30). PHF6-related hexapeptides having single amino acid substitutions (Ile → Val, Tyr → Ala, and Gln → Val) and N-terminal truncated analogs were prepared in order to study the filament-forming potential of these related structures. Because charge distribution has been shown to have a profound effect on the propensity of peptides to aggregate into filaments (51, 52), the peptides studied were prepared as *N*-acetylated peptide amides. In the absence of N- and C-terminal charges, the blocked peptides closely mimic peptide segments within the protein structure. Primary structures and molecular weights of peptides used are shown in Table I.

*Aggregation Kinetics*—AcPHF6KE, an analog of AcPHF6 with its positively charged C-terminal lysine replaced by a negatively charged glutamate, spontaneously formed a gel in distilled water or in the presence of strong hydrogen bond-breaking solvents (*i.e.* 99% formic acid or HFIP). All other *N*-acetylated peptide amides studied appeared soluble in distilled water but rapidly formed viscous solutions following the addition of NaCl.

We used the change in fluorescence upon binding of ThS to monitor the polymerization of peptide initiated by the addition

TABLE I
*Properties of peptides used in this study*

| Peptide | Sequence | Residues | $M_r$(calculated) | $M_r$ (observed) |
|---|---|---|---|---|
| PHF6 | H-VQIVYK-OH | 6 | 748.93 | 747.94 |
| AcPHF6 | Ac-VQIVYK-$NH_2$ | 6 | 789.98 | 790.10 |
| AcPHF6IV | Ac-VQVVYK-$NH_2$ | 6 | 775.95 | 776.43 |
| AcPHF6YA | Ac-VQIVAK-$NH_2$ | 6 | 697.88 | 701.39 |
| AcPHF6QV | Ac-VVIVYK-$NH_2$ | 6 | 760.58 | 761.20 |
| AcPHF6KE | Ac-VQIVYE-$NH_2$ | 6 | 790.92 | 791.60 |
| AcPHF5 | Ac-QIVYK-$NH_2$ | 5 | 690.85 | 690.84 |
| AcPHF4 | Ac-IVYK-$NH_2$ | 4 | 562.72 | 562.71 |
| AcVYK | Ac-VYK-$NH_2$ | 3 | 449.55 | 449.98 |
| AcYK | Ac-YK-$NH_2$ | 2 | 350.42 | 350.42 |

of NaCl to the buffered medium. Under these conditions unblocked PHF6 showed no aggregation within the experimental time frame. Initial polymerization kinetics for the remaining acetylated peptide amides (as shown in Fig. 1*A*) followed a single-exponential approach to equilibrium, consistent with a seeded nucleation-elongation mechanism (48). Similar kinetic behavior has been observed for polymerization of short amyloidogenic peptides and for heparin or arachidonic acid-catalyzed polymerization of tau constructs at high protein concentrations (18, 31, 46, 47, 53–55). At later times there was a deviation from single-exponential kinetic behavior for AcPHF4, likely as a result of the formation of higher order aggregates, and AcPHF6IV continued to show an increase in fluorescence, in a manner similar to that observed previously for transthyretin polymerization (56).

Apparent first-order rate constants are summarized in Table II. The results show that AcPHF6 had the most rapid aggregation rate and that the rate was decreased by N-terminal truncation. A plot of the logarithm of the apparent first-order rate constant as a function of the number of residues in the peptide (Fig. 1*B*) yielded a linear relationship ($r^2$ = 0.93). Changing Ile → Val or Gln → Val in the AcPHF6 sequence decreased the polymerization rate nearly 3-fold in comparison to AcPHF6, whereas changing Tyr → Ala decreased the rate nearly 10-fold.

*CD of Tau-related Peptides*—Fig. 2 shows the CD spectra of tau-related peptides in 5 mM MOPS buffer, pH 7.2. The CD spectra displayed by these peptides were of three types. Type A spectra, which had an intense negative band between 195 and 200 nm and a weak negative shoulder near 220 nm, are typical of proteins with a high fraction of random coil or polyproline II structure or of some $\beta_{II}$ proteins having a high fraction of truncated or twisted $\beta$-sheet structure (57–61). Peptides with type A spectra included AcPHF6YA, PHF6, and AcVYK. Type B spectra, typical of $\beta_I$ proteins and peptides having a high fraction of extended $\beta$-sheet structure, displayed a negative band near 217 nm and a positive band between 195 and 200 nm. Peptides that displayed a type B spectra included *N*-acetylated hexapeptides AcPHF6, AcPHF6IV, and AcPHF6QV. Type C spectra had some of the features of type B spectra but had additional bands that probably arose from the single tyrosine residue in the sequence. For example, AcPHF5 and AcPHF4 both had a negative band between 215 and 218 nm but only a slight positive band near 200 nm and an intense negative maximum near 190 nm. In addition to the bands below 200 nm, AcYK showed a positive band at 227 nm, most likely arising from the tyrosine $^1L_a$ band (62).

It has been demonstrated previously (56, 63) that both filamentous and soluble forms of amyloidogenic proteins contribute to their observed CD and that the fraction of aggregated forms may be estimated from the content of $\beta$-sheet structure. Although estimating secondary structure for short peptides in which there is a significant contribution to the CD from aromatic residues is difficult (57–64), our data show that peptides

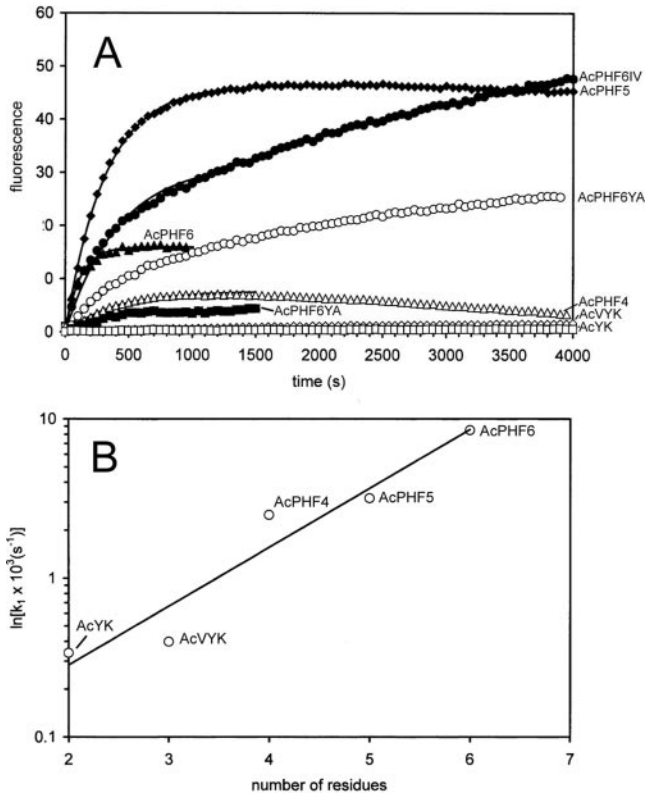


FIG. 1. *A*, kinetic data for the aggregation of tau-related peptides. Polymerization was initiated by the addition of NaCl (to 0.15 M) to a solution containing 2.2 $\mu$M peptide and 10 $\mu$M ThS in 20 mM MOPS buffer, pH 7.2 (21 °C), and was measured by the change in fluorescence at 480 nm (excitation 440 nm). Data were collected at a rate of 1 data point/s and fit over the first 2000 s to Equation 1 (*Solid line*). Data points are only shown every 100 s in order to simplify the appearance of the figure. *B*, the apparent first-order rate constant, $k_1$, is plotted against the number of residues in *N*-truncated AcPHF6 analogs. The *solid line* represents the best fit through the data points ($r^2$ = 0.93).

that display spectra more characteristic of random coil, such as PHF6, AcVYK, and AcPHF6YA, also have the slowest rates of polymerization. On the other hand, peptides that have rapid rates of polymerization, such as AcPHF6, AcPHF5, AcPHF4, AcPHF6QV, and AcPHF6IV, display CD spectra more characteristic of $\beta$-sheet (type B or C).

*FTIR Spectra of Tau-related Peptides*—Whereas the CD and ThS binding studies can be used to provide kinetic and structural information of the peptides in solution, FTIR can be used to provide structural information of fibrous peptides (65–68). Fig. 3 shows the amide I region of the FTIR spectra of AcPHF6, AcPHF5, AcPHF4, AcVYK, and AcYK in $D_2O$ (~10 mg/ml), and spectral parameters are summarized in Table III. The presence of significant helical or unordered structure in AcPHF6, AcPHF5, AcPHF4, and AcYK but not in AcVYK is inferred by bands contributing to the spectra in the region between 1645

TABLE II
*Parameters obtained from best fit of kinetic data*

Kinetic data were fit to the equation, $((I_t - I_0)/(I_f - I_0)) = 1 - e^{-k_1 t}$ where $I_f$ is the relative fluorescent intensity at infinite time; $k$ is the apparent first-order rate constant for addition of monomer to the growing polymer, and $I_0$ is the fluorescent intensity at time 0 (taken as zero after subtraction of the background). Numbers in parentheses are errors (95% confidence) determined from the least squares fit. PHF6 showed no measurable aggregation in the experimental time frame. PHF6KE showed extensive aggregation prior to the addition of NaCl and could not be measured.

| Peptide | $I_f - I_0$ | $k_1 \times 10^3$ s$^{-1}$ |
|---|---|---|
| AcPHF6 | 15.96 (±0.04) | 8.54 (±0.07) |
| AcPHF5 | 46.39 (±0.05) | 3.19 (±0.02) |
| AcPHF4 | 7.46 (±0.03) | 2.64 (±0.02) |
| AcVYK | 2.29 (±0.05) | 0.34 (±0.01) |
| AcYK | 0.99 (±0.02) | 0.31 (±0.01) |
| PHF6IV | 31.80 (±0.03) | 2.34 (±0.01) |
| PHF6YA | 25.44 (±0.02) | 0.86 (±0.01) |
| PHF6QV | 4.17 (±0.02) | 2.95 (±0.02) |

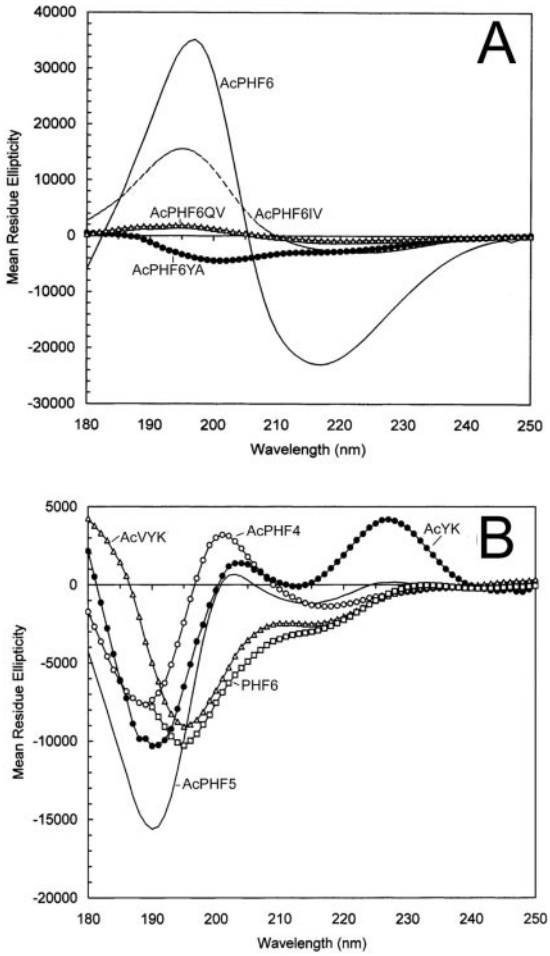


FIG. 2. **CD spectra of peptides in 5 mM MOPS buffer, pH 7.2.** Typically spectra were acquired on ~1 mg/ml peptides using a cell with a 0.2-mm path length following at least 4 days of aging at room temperature. *A*, peptides AcPHF6, AcPHF61V, AcPHF6QV, AcPHF6YA. *B*, peptides PHF6, AcPHF5, AcPHF4, AcVYK, AcYK.

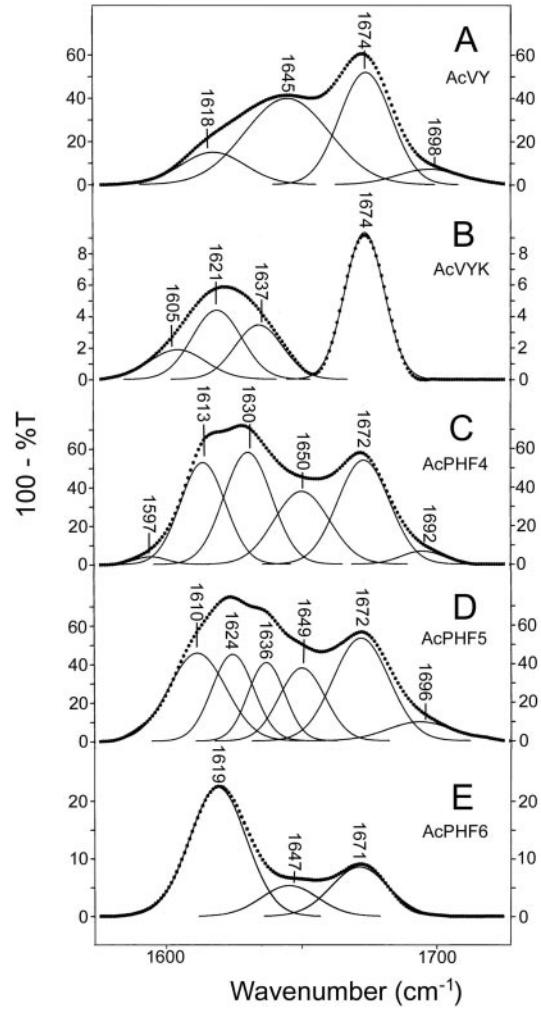


FIG. 3. **FTIR spectra in the amide I region of AcYK (*A*), AcVYK (*B*), AcPHF4 (*C*), AcPHF5 (*D*), and AcPHF6 (*E*) in $D_2O$ (~10 mg/ml).** Spectra were fit to Gaussian bands. Parameters are summarized in Table III. The band between 1670 and 1674 cm$^{-1}$ arises from trifluoroacetic acid, a contaminant of the high pressure liquid chromatography purification procedure.

and 1650 cm$^{-1}$. The spectra of AcVYK, AcPHF4, and AcPHF5 had multiple low frequency amide I bands between 1610 and 1637 cm$^{-1}$, suggesting that the β-sheet structure in these peptides exists in multiple aggregation states (69, 70). AcPHF6 and AcVYK were unique in that their IR spectra showed low frequency amide I bands between 1619 and 1637 cm$^{-1}$, characteristic of β-sheet, but no high frequency component between 1684 and 1704 cm$^{-1}$, characteristic of an antiparallel strand configuration. Hence, the data suggest that AcPHF6 and AcVYK have parallel β-sheet configuration.

*TEM of Tau-related Peptides*—TEM examination of all peptides longer than AcYK showed that they formed abundant filaments in water or MOPS buffer, pH 7.2. The filaments were composed of two parallel protofilaments, 5 ± 1 nm in width and 1–2 μm in length. Representative examples are shown in Fig. 4, *A–C*. Protofilaments of the tripeptide AcVYK appeared loosely associated with one another and frequently were seen as untwisted bundles. Although ribbon-like and fibrillar structures have been reported previously to be formed from tetra- and pentapeptides (71, 72), to our knowledge AcVYK is the shortest peptide yet reported capable of forming filaments.

Although a detailed time-dependent study was not undertaken, preliminary results suggest that filaments observed immediately after dissolution of AcPHF6 lyophilized powder were identical in morphology to filaments observed following several days of aging. These results were consistent with FTIR of the powder which showed prominent peaks in the 1610–1640 cm$^{-1}$ region, characteristic of β-sheet (data not shown).

Solutions of AcYK were estimated from CD and FTIR to contain β-sheet structure and also showed slow binding of ThS in kinetic studies. Therefore, we were hopeful of observing filaments formed from the dipeptide by TEM. Although we

TABLE III
*Fitted parameters for FTIR amide I bands*

Spectra were acquired at 2 $cm^{-1}$ resolution in $D_2O$ (~10 mg/ml). Results are for fits to Gaussian line widths. Numbers in parentheses represent integrated intensities.

| Peptides | Amide I band $cm^{-1}$ | | | | |
|---|---|---|---|---|---|
| PHF6 | | 1623 (16.4) | | 1645 (79.1) | 1700 (4.5) |
| AcPHF6 | | 1619 (84.1) | | 1647 (15.9) | |
| AcPHF6IV | | 1619 (84.1) | | 1647 (33.9) | 1697 (4.1) |
| AcPHF6YA | 1613 (32.8) | 1626 (42.2) | | 1647 (22.9) | 1685 (1.9) |
| AcPHF6QV | 1612 (28.9) | 1625 (38.0) | 1642 (16.7) | 1657 (9.8) | 1685 (6.6) |
| PHF5 | 1611 (28.9) | 1624 (25.1) | 1636 (20.1) | 1650 (22.8) | 1696 (3.1) |
| PHF4 | 1613 (27.9) | 1630 (36.5) | | 1650 (28.6) | 1692 (7.0) |
| AcPHF6KE[a] | 1608 (14.1) | | 1631 (56.5) | 1661 (26.8) | 1686 (2.6) |
| AcVYK | | 1621 (74.4) | 1635 (25.6) | | |
| AcYK | | 1618 (20.0) | | 1645 (70.5) | 1698 (9.5) |

[a] Prepared as a film from HFIP.

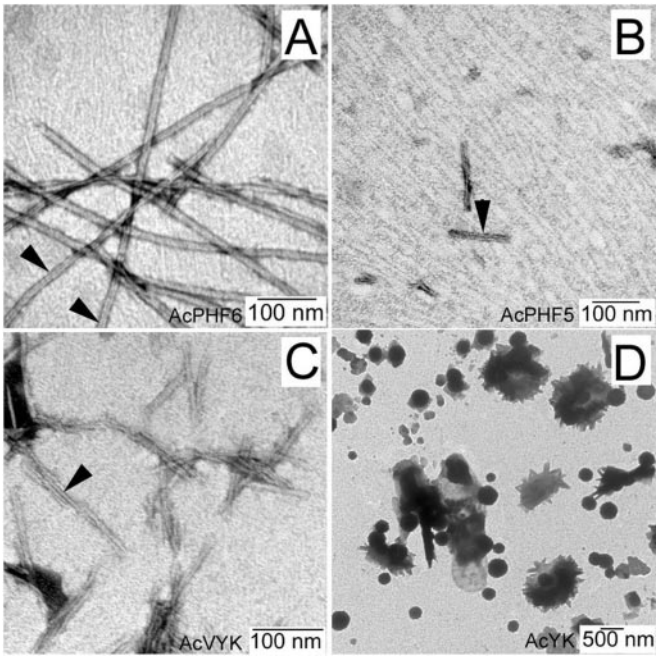


FIG. 4. **Transmission electron micrographs of AcPHF6, 0.4 mg/ml, in water, pH 6.8 (*A*); AcPHF5, 1 mg/ml, in 5 mM MOPS, pH 7.2 (*B*); AcVYK, 1 mg/ml, in water, pH 6.8 (*C*); and AcYK 4.4 mg/ml in 20 mM MOPS, pH 7.2, containing 0.15 M NaCl (*D*).** *Arrowheads* point to discernible protofilaments. Solutions were aged at least 2 days at room temperature (~21 °C) prior to sample preparation. TEM grids were negatively stained with 1% uranyl acetate.

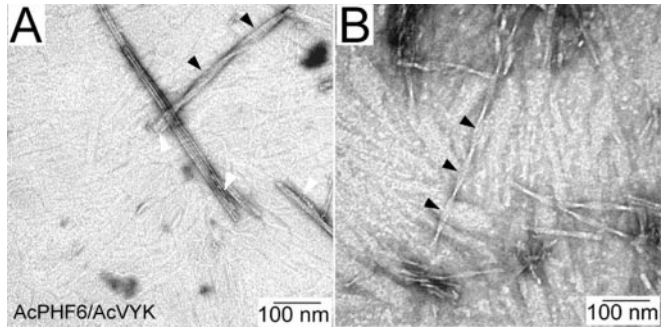


FIG. 5. **Transmission electron micrographs of twisted filaments formed from 0.32 mM AcPHF6 and 0.92 mM AcVYK in 5 mM MOPS, pH 7.2.** TEM grids were negatively stained with 1% uranyl acetate. *Black arrowheads* point to wide areas of twisted filaments. *A,* TEM prepared shortly after mixing. Four 6.7 ± 0.5 nm protofilaments are seen to align laterally to one another making a ribbon-like structure 27 ± 1 nm in width (*center* of panel). The ribbon-like structures begin to twist to form loosely twisted filaments with a width that varies between 8 ± 1 and 20 ± 2 nm and a half-periodicity of 153 ± 5 nm. Frayed protofilaments can be seen at the ends of the twisted filament structures (*white arrowheads*). *B,* filaments observed 2 days after mixing had a slightly tighter, more uniform twist with a width that varied between 8 ± 1 and 19 ± 1 nm and a half-periodicity of 94 ± 4 nm.

were unable to observe filaments, we did observe ~250-nm to 1-$\mu$m globules and spherical particles when samples were prepared from buffer containing 0.15 M NaCl (Fig. 4*D*).

*Twisted Filaments Prepared from Short Peptides*—It has been suggested that PHF6 interacts with another homologous sequence in the MBTR, PHF6*(VQIINK), to form a nucleus upon which twisted filaments are built (19, 30). Based on these findings, we attempted to form PHFs by mixing two different peptides, which individually formed straight amyloid-like filaments. Our hypothesis was that hydrogen-bonding interactions between the two peptide fragments would mimic similar interactions between sequences of tau distant from one another in the protein structure.

Fig. 5 shows filaments observed by TEM after mixing AcPHF6 with AcVYK tripeptide in MOPS buffer, pH 7.2. In Fig. 5*A*, obtained shortly after mixing, four 6.7 ± 0.5 nm protofilaments are seen to align laterally to one another making a ribbon-like structure 27 ± 1 nm in width (center of panel). These ribbon-like structures begin to twist to form loosely twisted filaments with a width that varies between 8 ± 1 and 20 ± 2 nm and a half-periodicity of 153 ± 5 nm. In some cases, frayed protofilaments can be seen at the ends of the twisted filament structures (Fig. 5*A*, *white arrowheads*). Filaments observed 2 days after mixing (Fig. 5*B*) had a slightly tighter, more uniform twist with a width that varied between 8 ± 1 and 19 ± 1 nm and a half-periodicity of 94 ± 4 nm. The morphology of these twisted filaments is similar to the morphology observed for PHFs that have a width that varies between 10 and 20 nm and a half-periodicity of 80 nm.

*X-ray Diffraction from Tau-related Peptides*—Diffraction patterns of tau-related peptides AcPHF6, AcPHF5, AcPHF4, and AcVYK from three different states of preparation (lyophilized, vapor-hydrated, and solubilized/dried) showed a sharp reflection at 4.7-Å spacing. In addition, solubilized/dried AcVYK, lyophilized AcPHF4, and solubilized/dried AcPHF6 showed ~10- and 3.8-Å reflections, which are characteristic of an orthogonal unit cell of the $\beta$-sheet, where the unit cell dimensions along the H-bonding, chain, and intersheet axes are $a$ = 9.4 Å, $b$ = 6.6 Å, and $c$ = ~10 Å (Fig. 6 and Table IV). These reflections were assigned Miller indices of (200) for 4.7 Å, (210) for 3.8 Å, and (001) for 10 Å. Peptide AcPHF5, which has Gln at its N terminus, did not show distinct 3.8- and 10-Å reflections, indicating that the $\beta$-sheets in these peptide assemblies may be limited in the intersheet and chain directions. All samples of AcVYK, AcPHF4, AcPHF5, and lyophilized and vapor-hydrated samples of AcPHF6 showed spherically averaged intensity, indicating that the scattering objects in these assemblies were distributed randomly. By contrast, solubilized/

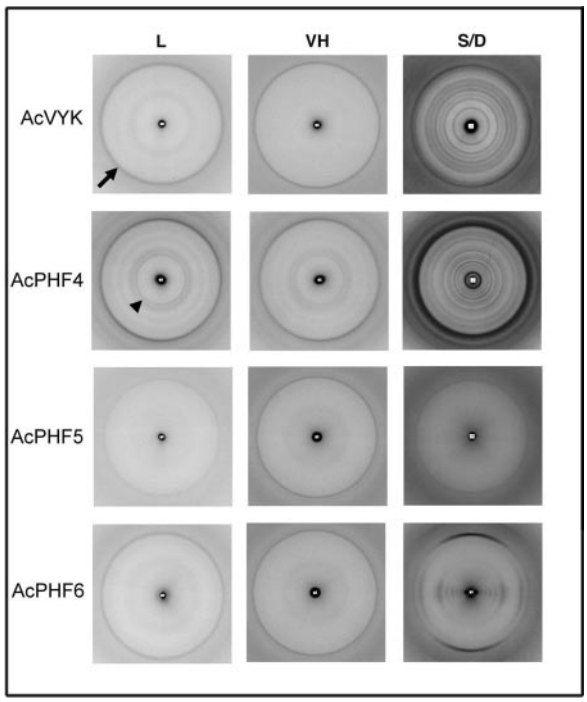


FIG. 6. **X-ray diffraction patterns from tau-related peptides AcVYK, AcPHF4, AcPHF5, and AcPHF6.** Peptide preparations all showed low angle reflections arising from a macro-lattice assembly. By contrast with the other peptides, AcPHF5 did not show abundant reflections. Peptides other than AcPHF6 gave spherically averaged intensities. *Arrow* and *arrowhead* indicate the 4.7- and ~10-Å spacings, respectively.

dried AcPHF6 gave oriented patterns showing cylindrically averaged intensity, as expected in fiber diffraction where the fiber axis is along the direction of the 4.7-Å reflection. Because the meridional axis was assumed to be along the H-bonding direction (vertical), the equatorial scatter was interpreted as arising from the packing of fibers. The ~10 Å-intersheet (001) reflection, however, was on the equator (*i.e.* normal to the fiber axis), and the (210) reflection at 3.8-Å spacing was off-meridional, on the 4.7-Å layer line. These reflections indicate that the $\beta$-chains were running nearly normal to the fiber direction, *i.e.* in "cross-$\beta$" arrangement. Because the peptides AcVYK, AcPHF4, and AcPHF5 gave spherically averaged powder diffraction rather than fiber diffraction patterns, their cylindrical axes (*i.e.* fibril direction) could not be determined experimentally. However, the sharpness of the 4.7-Å reflection indicated that the coherent domain size along the 4.7-Å H-bonding direction was large. Therefore, in these samples the scattering object was elongated along the H-bonding direction in the same way as in cross-$\beta$ structures.

In one or more of their hydration states, solubilized/dried AcVYK, lyophilized, and solubilized/dried AcPHF4 and solubilized/dried AcPHF6 all showed low angle reflections. The pattern of solubilized/dried AcVYK showed the reflection at 52 Å which may arise from the interference between the fibrils with the separation of 57 Å according to $52 \times 1.1$, where 1.1 came from the first intensity maximum of the $J_0$ Bessel term (73). The lyophilized AcPHF4 gave low angle concentric reflections that could be indexed by an apparent one-dimensional lattice of 64-Å periodicity arising from the periodic intensity maxima of a $J_0$ Bessel term (73). The solubilized/dried AcPHF6 gave an oriented diffraction pattern where the low angle equatorial reflections were indexed by an apparent one-dimensional lattice of 95-Å period. Of the peptides, AcPHF5 alone did not give a macro-assembly, suggesting that the Gln residue at the N terminus may preclude the longer range order required for such a structure.

## DISCUSSION

TEM results for all peptides, other than AcYK, showed that they formed filaments composed of two parallel protofilaments, each $5 \pm 1$ nm in width and 1–2 $\mu$m in length. In addition, x-ray diffraction data of AcPHF6 and for AcPHF5, AcPHF4, and AcVYK showed the omnipresent 4.7-Å reflection characteristic of the hydrogen bonding distance. The sharpness of this reflection likely indicates that the direction of the hydrogen bonding between $\beta$-chains is parallel to the fiber axis in a cross-$\beta$ conformation. Frequencies of amide I bands in the FTIR of AcPHF5 and AcPHF4 suggest that these peptides assume an antiparallel $\beta$-sheet configuration, whereas the spectra AcVYK and AcPHF6 suggest a parallel configuration. Both configurations have been observed previously in amyloid formed from other amyloidogenic peptides (74).

Although it has been shown previously (71, 72) that peptide sequences as short as a tetrapeptide are able to aggregate into filaments having an amyloid appearance, it was quite surprising to us that a peptide as short as a tripeptide was able to form amyloid. Furthermore, it is noteworthy that all peptides within the *N*-truncated AcPHF6 series produced ~50-Å wide protofilaments, independent of the length of the peptide chain. This suggests that at least in the case of the AcPHF6 peptides, protofilaments ~50 Å in width are especially stable. Because $\beta$-structure has a translation of 3.2–3.4 Å per residue, the peptide chains must either align end-to-end or partially overlap in a "brick wall" arrangement in order to span the width of the protofilament. A similar configuration of peptide chains has been proposed previously for amyloid peptidomimetics (75, 76).

We measured the polymerization kinetics of all PHF6-related peptides by following the binding of ThS, a flavin dye known to preferentially bind to peptide aggregates having cross-$\beta$ structure (45). All of the peptides, except for PHF6, were structurally similar in that they had a single uncompensated terminal charge at the C-terminal preceded by one or more N-terminal hydrophobic residues. It is noteworthy that all of the acetylated peptide amides aggregated with faster overall kinetics than the unblocked PHF6 peptide. This finding is in agreement with those of others who found that fibrils were only observed when the molecule carried a net charge of $\pm 1$ (51). One blocked peptide in which the C-terminal Lys was replaced by Glu, AcPHF6KE, formed viscous solutions in strong hydrogen bond-breaking solvents and was insoluble in aqueous media, suggesting that this peptide rapidly formed amyloid. All other *N*-acetylated peptide amides studied appeared soluble in distilled water but rapidly polymerized in the presence of 0.15 M NaCl. An enhanced rate of polymerization with increasing salt concentrations has been observed previously (51, 77) for other short amyloidogenic peptides and has been attributed to a lowered activation energy brought about by shielding of like charges on the peptide by counterions.

Frequently, conservative amino acid residue substitution or N-terminal truncation of short amyloid-forming peptides leads to amyloid incompetency (51–54, 72). This "all-or-none" effect has made it quite difficult to assess the contribution of individual amino acid residues to the amyloid forming potential of peptides and proteins. The AcPHF6 series of peptides, however, appear to be unique in their ability to tolerate structural changes and continue to form amyloid, albeit at a reduced rate. We have used kinetic parameters as a measure of "amyloid forming potential" in the same manner in which they have been used previously (18, 29–31, 34, 53, 54). We found that the rate of amyloid formation increased exponentially with the length of the peptide in going from AcYK → AcPHF6, independent of the

TABLE IV
*Summary of X-ray spacings*

The abbreviations used are as follows: C, circular; E, equator; M, meridian; M′, off meridian; vw, w, m, s, and vs indicate increasing intensity from very weak, weak, moderate, strong, to very strong. The low angle reflections likely arise from the β crystallites in a macromolecular array. The sample preparation is indicated by L for lyophilized, VH for vapor-hydrated, and S/D for solubilized and dried.

| AcVYK | | | AcPHF4 | | | AcPHF5 | | | AcPHF6 | | |
|---|---|---|---|---|---|---|---|---|---|---|---|
| L | VH | S/D | L | VH | S/D | L | VH | S/D | L | VH | S/D |
| 9.7[b] Cw | 4.7[a] Cs | 52 Cs | 32 Cw | 11 Cm | 60 Cw | 4.8[a] Cs | 9.1[b]Cw | 4.8[a] Cs | 44 Cm | 4.7[a] Cs | 95 Evs |
| 4.7[a] Cs | | 15 Cm | 17 Cw | 9.6[b]Cm | 36 Cs | | 4.8[a] Cs | | 8.5[b]Cw | | 47 Es |
| | | 10[b]Cm | 13 Cw | 7.0 Cw | 30 Cs | | 4.5 Cw | | 4.7[a] Cs | | 25 Evw |
| | | 8.8 Cw | 11[b]Cm | 5.7 Cw | 17 Cw | | | | 4.0 Cvw | | 18 Evw |
| | | 7.7 Cm | 9.4[b]Cm | 4.8[a] Cs | 14 Cw | | | | | | 14 Ew |
| | | 6.9 Cw | 6.9 Cw | 4.0 Cw | 8.7[b]Cw | | | | | | 11[b] Ew |
| | | 6.1 Cm | 5.6 Cw | 3.6 Cw | 6.3 Cw | | | | | | 8.2[b] Em |
| | | 5.0 Cw | 4.7[a] Cs | | 4.8[a] Cs | | | | | | 5.4 Em |
| | | 4.7[a] Cs | 4.4 Cw | | 4.1 Cm | | | | | | 4.7 Em |
| | | 4.2 Cw | 4.0 Cw | | 3.5 Cm | | | | | | 4.7[a] Ms |
| | | 3.9 Cw | 3.9 Cw | | | | | | | | 3.8 M′m |
| | | 3.3 Cm | 3.5 Cw | | | | | | | | |

[a] The characteristic reflections of β-sheet are indicated for H-bonding distance ~4.7 Å.
[b] Intersheet distance is ~10 Å.

type of residue added. The analogs in which one amino acid residue is substituted internally for another all showed decreased rates of polymerization relative to the parent hexapeptide. There is about a 3-fold decrease in the polymerization rate for AcPHF6IV and PHF6QV but nearly a 10-fold decrease in the rate of AcPHF6YA. The importance of Tyr and Phe residues in amyloidogenic peptide sequences has been attributed previously to favorable aromatic π-stacking interactions (34, 53, 54). However, a common motif in these short amyloidogenic peptides seems to be a series of hydrophobic residues followed by a polar or charged residue (72). The substitution of Tyr for Ala in AcPHF6YA results in a less hydrophobic side chain next to the charged Lys residue (78), leading to a reduced rate of polymerization.

Because polymerization in the absence of added NaCl was slow, the observed CD spectra reflect contributions of random coil peptides in solution and of β-sheet peptides in the pre-amyloid and amyloid states. Spectra of PHF6, AcPHF6YA, and AcVYK were characteristic of unordered structure (type A spectra), implying that a relatively small fraction of these peptides exists in a pre-amyloid or amyloid state. In contrast, peptides AcPHF4, AcPHF5, AcPHF6, AcPHF6IV, and AcPHF6QV polymerized more rapidly, and their spectra reflected a greater fraction of β-sheet structure (type B and type C spectra). These results suggest that the relative rates of polymerization in the presence of NaCl are preserved in its absence.

Although AcYK did not form filaments, it did form large crystalline-like spherical and globular structures similar to nonfibrous structures formed by tau (33), bovine phosphatidylinositol 3-kinase (38), $\beta_2$-microglobulin (37), and Aβ amyloid peptide (36, 39–42). These structures are frequently seen before the appearance of fibers, and it has been proposed that they are intermediates in amyloid formation (79). If it is assumed that the smallest nucleation site is a peptide of the general structure $(X)_nK$ (or $K(X)_n$), where $n \geq 2$ and $X$ is a residue frequently found in β-sheet, then there are several potential nucleation sites in tau that satisfy this criteria including $^{87}$KQAA$^{90}$, $^{225}$KVAVV$^{229}$, $^{274}$KVQII$^{278}$, $^{275}$VQIINK$^{280}$ (PHF6*), $^{305}$KVQIVY$^{310}$, $^{306}$VQIVYK$^{311}$ (PHF6), and $^{392}$IVYK$^{395}$. Of these PHF6*, PHF6, and longer peptides that include the sequence $^{392}$IVYK$^{395}$ are already known to form filaments (30, 80). If the criteria for a potential nucleus is broadened to include the general structure $(X)_nZ$ (or $Z(X)_n$), where $Z$ is a charged residue and $X$ is a residue frequently found in β-sheet, then the number of potential nuclei for amyloid formation in tau becomes much larger. Amyloidogenic nuclei in other protein fragments that form filaments also appear to follow this motif including NAGDVAFV (underlined sequences follow the $Z(X)_n$ motif) from lactoferrin (81), KLVFFAE (amphiphilic with charged residues at both ends) from Aβ peptide (82), and NFLVHSS from human islet amyloid polypeptide (54). The motif also serves as a basis for a family of other amyloid-forming hexapeptides (51).

Phosphorylation of threonine or serine in tau could potentially convert a polar amino acid into a charged amino acid, providing a mechanism for generating the $(X)_nZ$ motif, where $Z$ represents a charged phosphoserine or phosphothreonine. However, inspection of the tau sequence shows that serine and threonine residues do not occur near other residues predicted to form β-sheet ($X_n$). Instead, most occur near prolines, known β-sheet breakers or other charged residues. However, our results do not eliminate the possibility that other amyloidogenic nuclei can be generated upon serine or threonine phosphorylation in other proteins.

Our data show that mixtures of short peptides AcVYK and AcPHF6 produce twisted filaments with widths varying between 9 and 20 nm and a half-periodicity of 90 nm, similar in morphology to PHF. These results suggest that it is the interaction between amyloid nuclei in the tau sequence which leads to PHF morphology. This conclusion is consistent with previous findings that sequences remote from the MTBR, such as the N-terminal inserts and the C-tail of tau, may affect tau polymerization and filament morphology (33, 34).

One of our TEM images taken shortly after mixing AcPHF6 and AcVYK (Fig. 5*A*) provides some insight as to how PHF morphology is formed from protofilaments. The image shows four laterally arrayed protofilaments beginning to twist, creating a twisted ribbon morphology. In images taken 1 week after mixing, no filaments were found, suggesting that twisted filaments represent a metastable state. A similar disintegration of PHF-like filaments has been demonstrated for the full-length tau after aging (33). It is possible that *in vivo* PHFs are stabilized by other proteins or a unique PHF-associated glycolipid as we have found previously (83).

In summary, our results confirm previous findings that aromatic residues neighboring charged residues are particularly amyloidogenic (34, 53, 54, 72) and that very short amphiphilic peptide sequences may act as nuclei for amyloid formation. Twisted filaments were formed by mixing two amphiphilic peptides AcPHF6 and AcVYK, suggesting that the formation of PHFs is initiated by the interaction of two or more short amphiphilic sequences within tau and that long contiguous segments of the protein, *i.e.* the MTBR, are *not* necessary for twisted filament formation.

REFERENCES


1. Spillantini, M. G., Goedert, M., Crowther, R. A., Murrell, J. R., Farlow, M. R., and Ghetti, B. (1997) *Proc. Natl. Acad. Sci. U. S. A.* **94,** 4113–4118
2. Ksiezak-Reding, H., Morgan, K., Mattiace, L. A., Davies, P., Liu, W. K., Yen, S. H., Weidenheim, K., and Dickson, D. W. (1994) *Am. J. Pathol.* **145,** 1496–1508
3. Feany, M. B., and Dickson, D. W. (1996) *Ann. Neurol.* **40,** 139–148
4. Feany, M. B., Mattiace, L. A., and Dickson, D. W. (1996) *J. Neuropathol. Exp. Neurol.* **55,** 53–67
5. Dickson, D. W., Crystal, H. A., Bevona, C., Honer, W., Vincent, I., Davies, P. (1995) *Neurobiol. Aging* **16,** 285–298
6. Wischik, C. M., Crowther, R. A., Stewart, M., and Roth, M. (1985) *J. Cell Biol.* **100,** 1905–1912
7. Crowther, R. A., and Wischik, C. M. (1985) *EMBO J.* **4,** 3661–3665
8. Pollanen, M. S., Markiewicz, P., Bergeron, C., and Goh, M. C. (1994) *Am. J. Pathol.* **144,** 869–873
9. Lee, V. M. Y., Balin, B. J., Otvos, L., Jr., and Trojanowski, J. Q. (1991) *Science* **251,** 675–678
10. Kosik, K. S., and Greenberg, S. M. (1994) in *Alzheimer's Disease* (Terry, R. D., Katzman, R., and Bick, K. L., eds) pp. 335–344, Raven Press, Ltd., New York
11. Mandelkow, E.-M., Schweers, O., Drewes, G., Biernat, J., Gustke, N., Trinczek, B., and Mandelkow, E. (1996) *Ann. N. Y. Acad. Sci.* **777,** 96–106
12. Goedert, M., Wischik, C. M., Crowther, R. A., Walker, J. E., and Klug, A. (1988) *Proc. Natl. Acad. Sci. U. S. A.* **85,** 4051–4055
13. Khatoon, S., Grundke-Iqbal, I., and Iqbal, K. (1992) *J. Neurochem.* **59,** 750–753
14. Ksiezak-Reding, H., Liu, W. K., and Yen, S. H. (1992) *Brain Res.* **597,** 209–219
15. Kopke, E., Tung, Y. C., Shaikh, S., Alonso, A. C., Iqbal, K., Grundke-Iqbal, I. (1993) *J. Biol. Chem.* **268,** 24374–24384
16. Grundke-Iqbal, I., Iqbal, K., Tung, Y. C., Quinlan, M., Wisniewski, H. M., and Binder, L. I. (1986) *Proc. Natl. Acad. Sci. U. S. A.* **83,** 4913–4917
17. Schneider, A., Biernat, J., von Bergen, M., Mandelkow, E., and Mandelkow, E.-M. (1999) *Biochemistry* **38,** 3549–3558
18. Abraha, A., Ghoshal, N., Gamblin, T. C., Cryns, V., Berry, R. W., Kuret, J., and Binder, L. I. (2000) *J. Cell Sci.* **113,** 3737–3745
19. von Bergen, M., Barghorn, S., Li, L., Marx, A., Biernat, J., Mandelkow, E.-M., and Mandelkow, E. (2001) *J. Biol. Chem.* **276,** 48165–48174
20. Kirschner, D. A., Abraham, C., and Selkoe, D. J. (1986) *Proc. Natl. Acad. Sci. U. S. A.* **83,** 503–507
21. Berriman, J., Serpell, L. C., Oberg, K. A., Fink, A. L., Goedert, M., and Crowther, R. A. (2003) *Proc. Natl. Acad. Sci. U. S. A.* **100,** 9034–9038
22. Giannetti, A. M., Lindwall, G., Chau, M.-F., Radeke, M. J., Feinstein, S. C., and Kohlstaedt, L. A. (2000) *Protein Sci.* **9,** 2427–2435
23. Wischik, C. M., Novak, M., Thogersen, H. C., Edwards, P. C., Runswick, M. J., Jakes, R., Walker, J. E., Milstein, C., Roth, M., and Klug, A. (1988) *Proc. Natl. Acad. Sci. U. S. A.* **85,** 4506–4510
24. Jakes, R., Novak, M., Davison, M., and Wischik, C. M. (1991) *EMBO J.* **10,** 2725–2729
25. Wille, H., Drewes, G., Biernat, J., Mandelkow, E.-M., and Mandelkow, E. (1992) *J. Cell Biol.* **8,** 573–584
26. Schweers, O., Mandelkow, E.-M., Biernat, J., and Mandelkow, E. (1995) *Proc. Natl. Acad. Sci. U. S. A.* **92,** 8463–8467
27. Goedert, M., Jakes, R., Spillantini, M. G., Hasegawa, M., Smith, M. J., and Crowther, R. A. (1996) *Nature* **383,** 550–553
28. Crowther, R. A. (1991) *Proc. Natl. Acad. Sci. U. S. A.* **88,** 2288–2292
29. Li, L., von Bergen, M., Mandelkow, E.-M., and Mandelkow, E. (2002) *J. Biol. Chem.* **277,** 41390–41400
30. von Bergen, M., Friedhoff, P., Biernat, J., Heberle, J., Mandelkow, E.-M., and Mandelkow, E. (2000) *Proc. Natl. Acad. Sci. U. S. A.* **97,** 5129–5134
31. Barghorn, S., Zheng-Fischhofer, Q., Ackmann, M., Biernat, J., von Bergen, M., Mandelkow, E.-M., and Mandelkow, E. (2000) *Biochemistry* **39,** 11714–11721
32. Barghorn, S., and Mandelkow, E. (2002) *Biochemistry* **41,** 14885–14896
33. King, M. E., Gamblin, T. C., Kuret, J., and Binder, L. I. (2000) *J. Neurochem.* **74,** 1749–1757
34. Gamblin, T. C., Berry, R. W., and Binder, L. I. (2003) *Biochemistry* **42,** 2252–2257
35. Ishimaru, D., Andrade, L. R., Teixeira, L. S. P., Quesado, P. A., Maiolino, L. M., Lopez, P. M., Cordeiro, Y., Costa, L. T., Heckl, W. M., Weissmuller, G., Foguel, D., and Silva, J. L. (2003) *Biochemistry* **42,** 9022–9027
36. Hoshi, M., Sato, M., Matsumoto, S., Noguchi, A., Yasutake, K., Yoshida, N., and Sato, K. (2003) *Proc. Natl. Acad. Sci. U. S. A.* **100,** 6370–6375
37. Kad, N. M., Myers, S. L., Smith, D. P., Smith, D. A., Radford, S. E., and Thomson, N. H. (2003) *J. Mol. Biol.* **330,** 785–797
38. Bucciantini, M., Giannoni, E., Chiti, F., Baroni, F., Formigli, L., Zurdo, J., Taddei, N., Ramponi, G., Dobson, C. M., and Stefani, M. (2002) *Nature* **416,** 507–511
39. Lashuel, H. A., Hartley, D. M., Petre, B. M., Wall, J. S., Simon, M. N., Walz, T., and Lansbury, P. T., Jr. (2003) *J. Mol. Biol.* **332,** 795–808
40. Huang, T. H. J., Yang, D.-S., Plaskos, N. P., Go, S., Yip, C. M., Fraser, P. E., and Chakrubartty, A. (2000) *J. Mol. Biol.* **297,** 73–87
41. Huang, T. H. J., Yang, D.-S., Fraser, P. E., and Chakrabartty, A. (2000) *J. Biol. Chem.* **275,** 36436–36440
42. Choma, C. T., Lear, J. D., Nelson, M. J., Dutton, P. L., Robertson, D. E., and DeGrado, W. F. (1994) *J. Am. Chem. Soc.* **116,** 856–865
43. Edelhock, H. (1967) *Biochemistry* **6,** 1948–1954
44. Gill, S. C., and von Hippel, P. H. (1989) *Anal. Biochem.* **182,** 319–326
45. LeVine, H., III (1993) *Protein Sci.* **2,** 404–410
46. Friedhoff, P., Schneider, A., Mandelkow, E.-M., and Mandelkow, E. (1998) *Biochemistry* **37,** 10223–10230
47. Friedhoff, P., von Bergen, M., Mandelkow, E.-M., Davies, P., and Mandelkow, E. (1998) *Proc. Natl. Acad. Sci. U. S. A.* **95,** 15712–15717
48. Inouye, H., and Kirschner, D. A. (2000) *J. Struct. Biol.* **130,** 123–129
49. Oldenbourgh, R., and Phillips, W. C. (1986) *Rev. Sci. Instrum.* **57,** 2362–2365
50. Makowski, L. (1989) in *Brookhaven Symposium: Synchrotron Radiation in Biology* (Sweet, R. M., and Woodhead, A. D., eds) pp. 341–347, Plenum Publishing Corp., New York
51. Lopez de la Paz, M., Goldie, K., Zurdo, J., Lacroix, E., Dobson, C. M., Hoenger, A., and Serrano, L. (2002) *Proc. Natl. Acad. Sci. U. S. A.* **99,** 16052–16057
52. Caplan, M. R., Schwartzfarb, E. M., Zhang, S., Kamm, R. D., and Lauffenburger, D. A. (2002) *Biomaterials* **23,** 219–227
53. Azriel, R., and Gazit, E. (2001) *J. Biol. Chem.* **276,** 34156–34161
54. Mazor, Y., Gilead, S., Benhar, I., and Gazit, E. (2002) *J. Mol. Biol.* **322,** 1013–1024
55. Liu, R., McAllister, C., Lyubchenko, Y., and Sierks, M. R. (2004) *J. Neurosci. Res.* **75,** 161–171
56. MacPhee, C. E., and Dobson, C. M. (2000) *J. Mol. Biol.* **297,** 1203–1215
57. Woody, R. W. (1996) in *Circular Dichroism and the Conformational Analysis of Biomolecules* (Fasman, G. D., ed) pp. 25–67, Plenum Publishing Corp., New York
58. Manavalan, P., and Johnson W. C., Jr. (1987) *Anal. Biochem.* **167,** 76–85
59. Wu, J., Yang, J. T., and Wu, C.-S. C. (1992) *Anal. Biochem.* **200,** 359–364
60. Sreerama, N., and Woody, R. W. (2003) *Protein Sci.* **12,** 384–388
61. Manning, M. C., Illangasekare, M., and Woody, R. W. (1988) *Biophys. Chem.* **31,** 77–86
62. Goux, W. J., and Hooker, T. M., Jr. (1980) *J. Am. Chem. Soc.* **102,** 7080–7087
63. Goux, W. J. (2002) *Biochemistry* **41,** 13798–13806
64. Sreerama, N., and Woody, R. W. (2000) *Anal. Biochem.* **287,** 252–260
65. Krimm, S., and Bandekar, J. (1986) *Adv. Protein Chem.* **38,** 181–364
66. Haris, P. I., and Chapman, D. (1995) *Biopolymers* **37,** 251–263
67. Bandekar, J. (1992) *Biochim. Biophys. Acta* **1120,** 123–143
68. Venyaminov, S. Y., and Kalnin, N. N. (1990) *Biopolymers* **30,** 1259–1271
69. Zurdo, J., Guijarro, J. I., Jimenez, J. L., Saibil, H. R., and Dobson, C. M. (2001) *J. Mol. Biol.* **311,** 325–340
70. Zurdo, J., Guijarro, J. I., and Dobson, C. M. (2001) *J. Am. Chem. Soc.* **123,** 8141–8142
71. Tenidis, K., Waldner, M., Bernhagen, J., Fischle, W., Bergmann, M., Weber, M., Merkle, M.-L., Voelter, W., Brunner, H., and Kapurniotu, A. (2000) *J. Mol. Biol.* **295,** 1055–1071
72. Reches, M., Porat, Y., and Gazit, E. (2002) *J. Biol. Chem.* **277,** 35475–35480
73. Inouye, H., Fraser, P. E., and Kirschner, D. A. (1993) *Biophys. J.* **64,** 502–519
74. Rochet, J. C., and Lansbury, P. T., Jr. (2000) *Curr. Opin. Struct. Biol.* **10,** 60–68
75. West, M. W., Wang, W., Patterson, J., Mancias, J. D., Beasley, J. R., and Hect, M. H. (1999) *Proc. Natl. Acad. Sci. U. S. A.* **96,** 11211–11216
76. Lashuel, H. A., LaBrenz, S. R., Woo, L., Serpell, L. C., and Kelly, J. (2000) *J. Am. Chem. Soc.* **122,** 5262–5277
77. Caplan, M. R., Moore, P. N., Zhang, S., Kamm, R. D., and Lauffenburger, D. A. (2000) *Biomacromolecules* **1,** 627–631
78. Pace, C. N. (1995) *Methods Enzymol.* **259,** 538–554
79. Nybo, M., Svehag, S. E., and Holm, N. E. (1999) *Scand. J. Immunol.* **49,** 219–223
80. Yanagawa, H., Chung, S.-H., Ogawa, Y., Sato, K., Shibata-Seki, T., Masai, J., and Ishiguro, K. (1998) *Biochemistry* **37,** 1979–1988
81. Nilsson, M. R., and Dobson, C. M. (2003) *Biochemistry* **42,** 375–382
82. Balbach, J. J., Ishii, Y., Antzutkin, O. N., Leapman, R. D., Rizzo, N. W., Dyda, F., Reed, J., and Tycko, R. (2000) *Biochemistry* **39,** 13748–13759
83. Goux, W. J., Rodriguez, S., and Sparkman, D. R. (1996) *J. Neurochem.* **67,** 723–733


Protein Structure and Folding:

# The Formation of Straight and Twisted Filaments from Short Tau Peptides

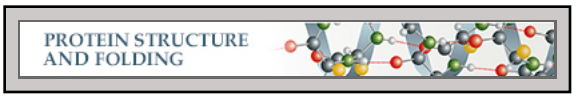


Warren J. Goux, Lauren Kopplin, Anh D. Nguyen, Kathryn Leak, Marni Rutkofsky, Vasanthi D. Shanmuganandam, Deepak Sharma, Hideyo Inouye and Daniel A. Kirschner

*J. Biol. Chem. 2004, 279:26868-26875.*
*doi: 10.1074/jbc.M402379200 originally published online April 20, 2004*

---